

# National Aeronautics and Space Administration

*As part of its mission to understand and protect the home planet, the Earth Science Enterprise at NASA supports various research programs in the Arctic that emphasize space-based and airborne remote sensing studies to characterize, understand, and predict changes in the Arctic and to examine their interactions with the rest of the Earth System.*

## Arctic Warming

Recent satellite thermal-infrared data have provided surface temperatures from 1981 to 2001, revealing large warming anomalies in the 1990s, compared to the decade before, along with a regional variability in the trends. These compare favorably with coincident in-situ measurements. Average temperature trends were generally positive, with sea ice warming by about a third of a degree Celsius per decade, Eurasia warming by about half a degree Celsius, and northern North America warming by nearly a degree Celsius. The trend is slightly negative but insignificant in Greenland ( $-0.09 \pm 0.25^\circ\text{C}$  per decade), with the negatives mainly at high elevations. The trends are also predominantly positive in spring, summer, and autumn, causing the lengthening of the melt season by 10–17 days per decade, while they are generally negative in winter. The longer-term in-situ surface temperature data show that the 20-year trend is eight times larger than the 100-year trend, suggesting a rapid acceleration in the warming that may be associated with the recent change in phase of the Arctic Oscillation, which has been linked to increasing greenhouse gases in the atmosphere.

## Sea Ice

### *Observing and Understanding Changes*

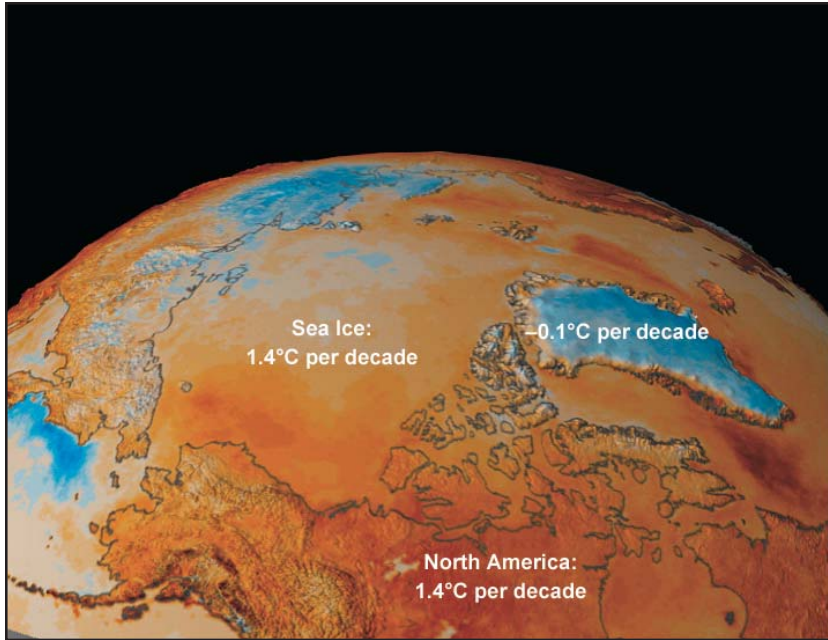
For many decades, explorers have sought a Northwest and Northeast Passage with a view of finding a sea route that would greatly shorten the link between East and West. These efforts have so far generally failed; some had horrific ends, mainly because of the dominant presence of the perennial sea ice cover, which consists mainly of multiyear ice, the average thickness of which is about 3 m. These thick, multiyear ice floes are the major components of the Arctic sea ice cover as we know it

	Funding (thousands)	
	FY 02	FY 03
Polar Ice Interactions	4,000	4,700
Terrestrial Ecology	510	710
Solid Earth Sciences	4,200	4,200
Hydrological Sciences	370	420
Modeling	250	250
Arctic Ozone	6,500	7,000
Clouds and Radiation	500	580
Suborbital Sciences	2,500	2,500
Physical Oceanography	200	570
Biological Oceanography	150	150
Satellite Algorithms/Data Analysis	6,000	6,000
Data Systems	11,000	9,500
Total	36,180	36,580

today. These floes survive the summer melt mainly because of a strongly stratified Arctic Ocean that is in part responsible for the scarcity of convection in the region. Historically the Northern Hemisphere winter sea ice cover consists of almost an even contribution of seasonal and perennial ice cover, with the former found primarily in the peripheral seas. A drastic change in this balance in favor of the former would mean an entirely different Arctic climate system and environment.

Analysis of satellite data from 1978 to 2002 showed a decrease in perennial Arctic sea ice cover of nearly 10% per decade, which is consistent with the observed Arctic warming and the lengthening of the melt season. A sustained decline at this rate would mean the disappearance of the multiyear ice cover during this century, which has been predicted by some climate models, along with potentially drastic changes in the Arctic climate system. The pressing question is whether these losses will slow down, reverse, or accelerate, which is a focus of ongoing activities.

A longer 30-year satellite record of sea ice extents, derived mostly from satellite microwave radiometer observations, reveals that the Arctic sea ice extent decreased by  $0.30 \pm 0.03 \times 10^6 \text{ km}^2$  per decade from 1972 through 2002, but by  $0.36 \pm 0.05 \times$



Arctic temperature trends derived from 20 years of satellite data.

$10^6 \text{ km}^2$  per decade from 1979 through 2002, indicating an acceleration of 20% in the rate of decrease. In contrast, the Antarctic sea ice extent decreased dramatically over the period 1973–1977, then gradually increased. Over the full 30-year period, the Antarctic ice extent decreased by  $0.15 \pm 0.08 \times 10^6 \text{ km}^2$  per decade. The trend reversal is attributed to a large positive anomaly in Antarctic sea ice extent in the early 1970s, an anomaly that apparently began in the late 1960s, as observed in early visible and infrared satellite images.

A new tool, the RADARSAT Geophysical Processor System (RGPS), produces high-resolution estimates of sea ice motion and deformation from time-sequential synthetic aperture radar (SAR) imagery acquired by RADARSAT. This data set provides observations over a spatial scale ranging from kilometers to thousands of kilometers (the Arctic Basin). More than four years (from November 1996 on) of RADARSAT acquisitions have been processed into geophysical fields of small-scale ice displacements. Although these records are not as long as their passive microwave counterparts, they allow a detailed look at deformation and motion processes of sea ice on large spatial scales.

A recent investigation, using a specially acquired RADARSAT data set, examined the properties of sub-daily ice motion of the sea ice cover. A persistent level of oscillatory sea ice motion and deformation was superimposed on the large-scale wind-driven field in May 2002 (spring) and February 2003 (mid-winter) in the high Arctic over a

region centered at approximately  $85^\circ\text{N}$ ,  $135^\circ\text{W}$ . At this latitude the RADARSAT wide-swath SAR coverage provides four or five sequential observations every day, for ice motion retrieval, with a sampling interval at the orbital period of approximately 101 minutes. The observed motions and deformation characteristics offer remarkable new insights into sea ice processes, as short-period ice motion was previously believed to be inhibited by the strength of the ice pack in the high Arctic during winter. New ice production due to the recurrent openings and closings at these temporal scales, if ubiquitous, could be significant within the winter pack. A simple simulation of this process shows that it can account for an equivalent of 10 cm of ice thickness over six months of winter, approximately 20% of the basal ice growth of thick ice in the central Arctic (of approximately 0.5 m).

#### Linking Observations to Models

NASA is continuing to contribute to climate research by encouraging international cooperation and the synergistic use of models and satellite observations. A collaborative study involving the NASA Goddard Institute of Space Studies and the UK's Hadley Centre is using the complementary strengths of two global circulation models to compare key drivers of Arctic climate under control and anthropogenic warming scenarios. Under pre-industrial atmospheric conditions in HadCM3, the spatial pattern of sea ice variability appears to be determined by the atmospheric heat flux (77% of the variance in ice concentration) and variability in the northward transport of heat in the North Atlantic Ocean (42%), the latter with a lag of a year to the heat flux at  $70^\circ\text{N}$ , and together accounting for 82% of the variance. Under a global warming scenario, the atmospheric heat flux becomes increasingly important, explaining 95% of the Arctic sea ice variance under  $4\times\text{CO}_2$  conditions. Runs with the new NASA GISS Model E are being used to establish whether incorporation of the full stratosphere and more sophisticated sea ice thermodynamics confirms this situation and provides detail on changes in key atmospheric processes in a climate change scenario, as well as to provide the framework for comparisons with 30 years of satellite observations of the Arctic.

#### Satellite Calibration and Validation

On May 4, 2002, the Advanced Microwave Scanning Radiometer (AMSR-E) developed by the National Space Development Agency (NASDA) of Japan was successfully launched on NASA's EOS

Aqua spacecraft. This new state-of-the-art satellite radiometer provides a wider range of frequencies and twice the spatial resolution than is currently available with the Defense Meteorological Satellite Program Special Sensor Microwave/Imager. The standard AMSR-E sea ice products include sea ice concentrations at spatial resolutions of 12.5 and 25.0 km, snow depth on sea ice at a spatial resolution of 12.5 km, and sea ice temperature at a spatial resolution of 25 km. The scientific usefulness of these products depends on their level of accuracy, which will be determined through the implementation of a sea ice product validation program consisting of three elements: satellite data comparisons, coordinated satellite/aircraft/surface comparisons, and a modeling and sensitivity analysis.



*The NASA Wallops P-3B aircraft at Fairbanks International Airport. The P-3, equipped with high-resolution sensors, obtained validation data as part of the EOS Aqua AMSR-E Arctic sea ice validation campaign. The same platform has been used regularly to survey changes in Arctic land ice elevations.*

The main objective of the AMSR-E sea ice validation program is to establish statistical relationships between the sea ice parameters derived from the new AMSR-E sea ice algorithms and those same parameters derived from other data sets obtained from satellite, aircraft, and surface-based measurements covering as many different sea ice conditions as possible for the purpose of providing a comprehensive measure of accuracy for each product. Other objectives are to understand the limitations of each of the AMSR-E sea ice algorithms, including the reasons for their particular level of performance under different conditions, and to suggest improvements to each of the algorithms based on the results of the validation studies.

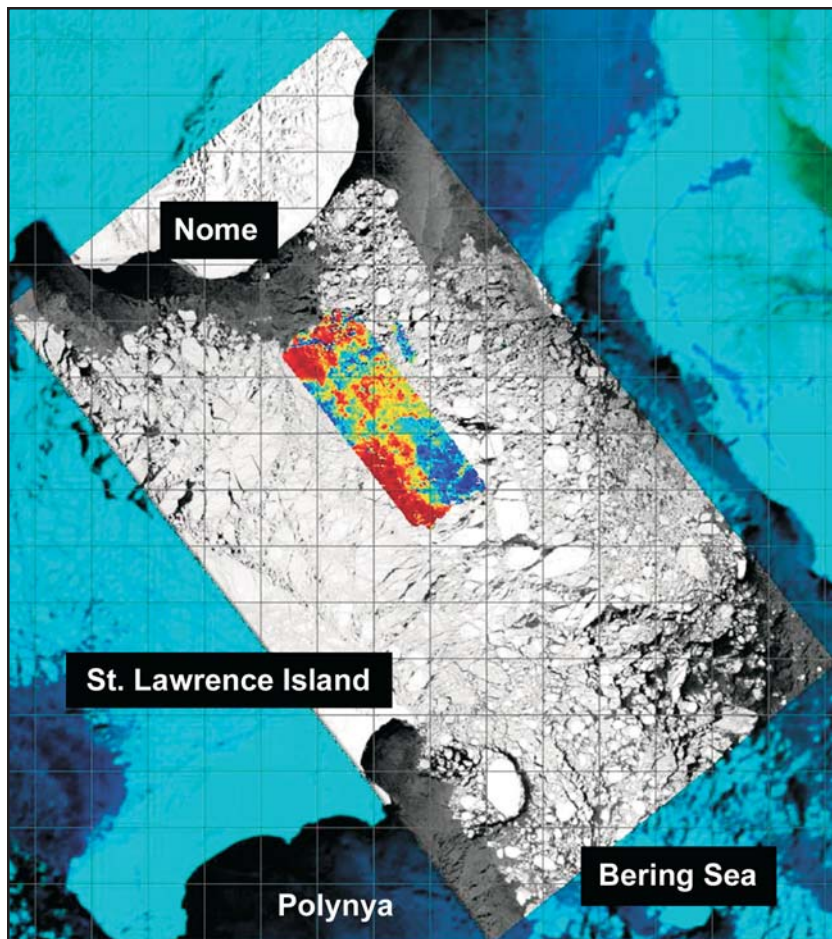
Arctic2003, the first of two coordinated Arctic satellite/aircraft/surface campaigns, was completed in March 2003. Seven flights were made with the NASA Wallops P-3B aircraft, covering portions of the Bering, Beaufort, and Chukchi Seas. Two of the seven aircraft flights were coordinated with scientists making surface measurements of snow and ice properties, including sea ice temperature and snow depth on sea ice at a study area near Barrow, Alaska, and at a Navy ice camp located in the Beaufort Sea. Two additional flights were dedicated to making heat and moisture flux measurements over the St. Lawrence Island polynya to support ongoing air-sea-ice process studies of Arctic coastal polynyas. The remaining flights covered portions of the Bering Sea ice edge, the Chukchi Sea, and Norton Sound.

The Arctic2003 aircraft flights also supported ongoing air-sea-ice process studies of Arctic coastal polynyas. The prime objective of the polynya flights is to assess the accuracy to which the AMSR-E sea ice concentration algorithms can map the size of coastal polynyas and to measure the degree of low ice concentration bias, if any, resulting from the presence of thin ice. A second objective is to directly measure surface heat and moisture fluxes over coastal polynyas to evaluate the parameterizations currently used in bulk formulation models and to measure the falloff of these fluxes downwind as the sea ice concentration and ice thickness increase.

## *Land Ice*

### *The Greenland Ice Sheet*

The primary focus of NASA's Arctic land ice research has been on assessing and understanding the mass balance of the Greenland ice sheet. Repeat surveys by airborne laser altimetry in the 1990s have revealed significant thinning of outlet glaciers draining the interior of the Greenland ice sheet, with thinning rates up to several meters per year. Of particular interest have been recent changes in the Jakobshavn ice stream, Greenland's main drainage system and most active outlet glacier, with an annual discharge of about 30 km<sup>3</sup> of ice. It is one of the few recently surveyed glaciers to thicken between 1993 and 1998, despite locally warm summers. Repeated airborne laser altimeter surveys along a 120-km profile in the glacier basin show slow, sporadic thickening between 1991 and 1997, suggesting a small positive mass balance. However, since 1997 there has been sustained thinning of several meters per



*PSR-A multicolor mosaic of a portion of the Bering Sea, from a NASA P-3 flight using the NOAA ETL PSR-A, overlain on a Landsat 7 ETM+ image (black and white), both for 15 March 2003. The Landsat image is centered on a NOAA-17 AVHRR image (blue). A 25-km AMSR-E grid is also shown for comparison. Polynyas are visible south of Nome, Alaska, and St. Lawrence Island.*

year within 20 km of the ice front, with lower rates of thinning farther inland. Here, weather station data from the coast and the ice sheet were used to estimate the effects on surface elevation of inter-annual variability in snowfall and surface melt rates to infer the temporal and spatial patterns of dynamic thinning. These show the glacier to have been close to balance before 1997, followed by a sudden transition to rapid thinning, initially confined to lower reaches of the glacier (below about 500-m elevation), but progressively spreading inland. Between 1999 and 2001, thinning predominated over the entire surveyed region up to 2000-m elevation. If this continues, the glacier calving front, and probably its grounding line, will retreat substantially in the near future.

Observations between 1997 and 2001, showing a 30% velocity increase and up to 60 m of thinning of downstream parts of Jakobshavn Isbrae immediately following calving of about 4 km of its 15-km floating ice tongue, suggest that acceleration may have been initiated by the calving and that the force perturbation associated with such weakening is swiftly transmitted far up-glacier. Initially

the observed changes are consistent with the comparatively small perturbation associated with the calving. Thereafter, it was probably sustained by thinning of the remaining ice tongue at rates of about 80 m per year. Otherwise, the force perturbation would soon have been balanced by reduction in the hydrostatic driving force for longitudinal creep as the glacier thinned, with velocities dropping to their former values. The calculated force perturbation increases to a maximum about 10 km inland of the grounding line, consistent with decreasing weight forces as the glacier thins over bedrock that slopes uphill seawards. Farther inland, it progressively decreases, probably because marginal drag increased as the glacier accelerated. Both here and on the floating tongue, marginal ice appears to have been softened by the influence of locally intense shear on ice temperature and/or fabric. More recent observations show continued acceleration and thinning, and most of the remaining ice tongue calved away in April 2003. Thus, thinning is likely to continue.

To fully appreciate the significance of these recent changes in Jakobshavn and other outlet glaciers, the magnitude of retreat and surface lowering must be placed within the broader context of retreat since the Last Glacial Maximum and, more significantly, retreat following the temporary glacier advance during the Little Ice Age (LIA). The instrumental record of glacier observations in Greenland dates back to aerial photography conducted by the Danes in the 1930s and 1940s. Glacier histories extending farther back in time must be based on geological information retrieved from formerly glaciated regions. In particular, the LIA maximum stand is marked by trimlines, a sharp boundary between unvegetated rocks recently deglaciated and vegetated surfaces at higher elevations.

To evaluate whether multispectral satellite images can be used to map trimlines and to distinguish different surface types, a Landsat ETM+ image of Jakobshavn Isbrae and vicinity was acquired. Applying supervised classification, thirteen surface types were identified, ranging from bare ice, debris-covered ice, and open water, to different types of vegetative cover. Each surface type is characterized by its spectral reflectance curve. To support the interpretation of the various surface classes, field measurements were conducted during July 2003 at three camps near the ice margin. Spectra of typical landcovers (mosses, lichen, sand and gravel, freshly deposited sediments,

etc.) were measured in the spectral range from 350 to 2500 nm, thus including the six Landsat spectral bands. Spectra measured in the field were compared to spectra of the thirteen classified surfaces to validate our interpretation of these classes.

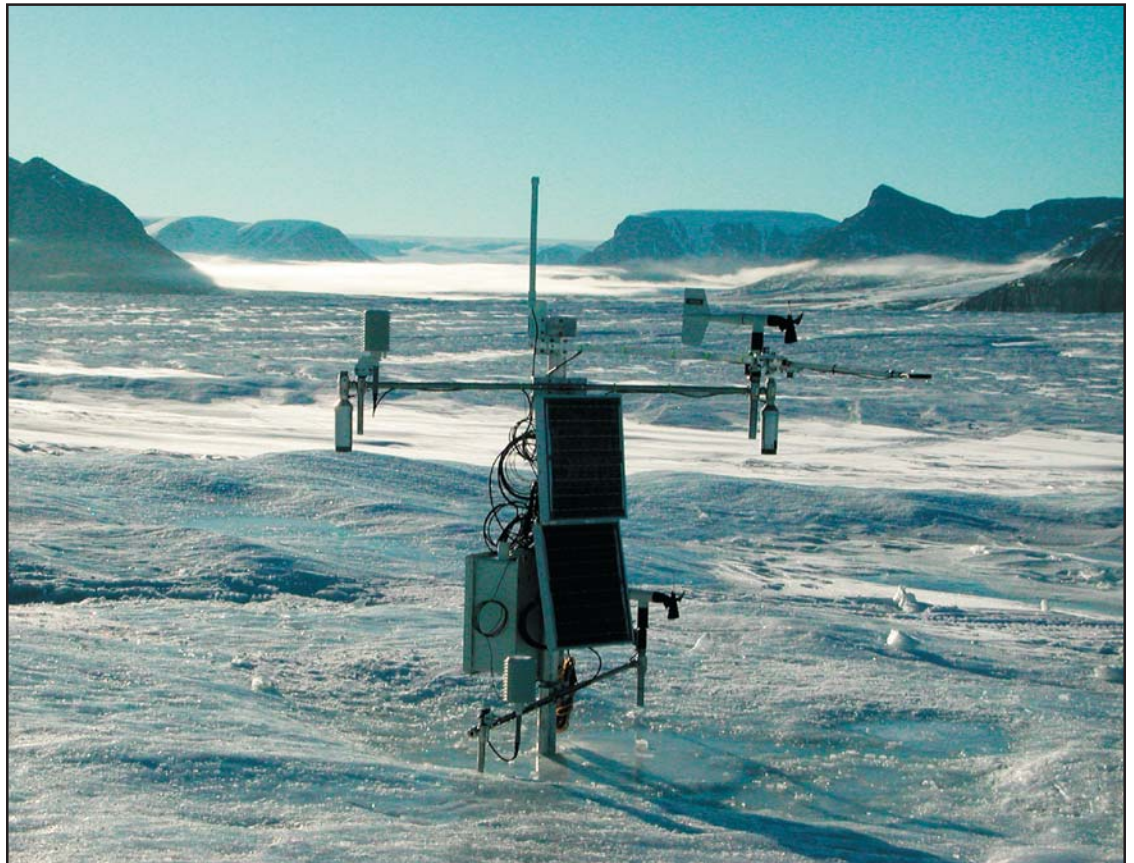
While in the field, moraine mapping was conducted with the intent to evaluate whether geomorphological landforms can be identified on satellite images. Unexpectedly, at the camp on the northern margin of the ice fjord, inspection of the surface below the trimline revealed a succession of lateral moraines consisting of boulders, gravel, and sand. These moraines were most likely formed at times when the ice margin was stationary or slowly changing, so each moraine signifies a period since the LIA during which the general trend of glacier thinning was interrupted. Accurately mapping these moraines involved extending a profile line from the trimline to the margin of the fjord ice for geomorphological mapping, and surveying it using a global positioning system and optical leveling to obtain accurate elevations. Also, along this profile, sizes of various lichen species were measured in an attempt to establish a dating curve. To assign ages to lichens of given size, a calibration curve was derived by measuring lichen

sizes on surfaces of known exposure date in the town of Ilulisat. Further analysis of these data is in the process, but preliminary interpretation suggests that thinning of Jakobshavn Isbræ since the LIA occurred intermittently. Interestingly, periods of thinning do not correlate in a simple way with retreat of the calving terminus.

To enable the interpretation of changes observed by remote sensing measurements, NASA established the Greenland Climate Network (GC-Net), a network of 18 automatic weather stations (AWSs) and five smart stakes (less sophisticated AWSs with measurements at one level only) distributed over the entire Greenland ice sheet. Four stations are located along the crest of the ice sheet (at elevations ranging from 2,500 to 3,200 m) in a north-south direction, ten stations are located close to the 2,000-m contour line (1,830–2,500 m), and four stations are positioned in the ablation region (560–1,150 m).

The GC-Net was established in the spring of 1995 with the intention of monitoring climatological and glaciological parameters at various locations on the ice sheet for at least 10 years. The first AWS was installed at the Swiss Camp, followed by four AWSs in 1995, four in 1996, five in

*Automatic weather station  
at Petermann Glacier  
(part of a joint project  
with the National Science  
Foundation described in  
the NSF section).*



1997, four in 1999, one in 2002, and two in 2003. Some were temporary, and 18 remain functioning on a quasi-permanent basis. The objectives for the Greenland weather station network are to measure daily, annual, and interannual variability in accumulation rate, surface climatology, and surface energy balance at selected locations on the ice sheet and to measure near-surface snow density at the AWS locations for the assessment of snow densification, accumulation, and metamorphosis.

Currently 630 parameters are transmitted every hour, and until a site is revisited, transmitted data are used. All the AWS sites are revisited within 2–3 years depending on logistics and accumulation. Statistical procedures are applied to the GC-Net data in effort to improve data quality. These include rejecting impossible values and using a gradient threshold comparing the measurement with the next sequential hourly value. A moving sample interval scans the time series to identify and reject data beyond a variance threshold for a given sample size. In some cases a spectrum of window sizes is employed to reject outliers caused by occasional data scrambling by transmission errors. In general, the data that are rejected by these filters represent a minor fraction of the data volume. Once a station is revisited, continuous data are retrieved to replace the transmitted data.

An annual mean latitudinal temperature gradient of  $-0.78^{\circ}\text{C}$  per  $1^{\circ}$  of latitude was derived from the AWS data for the western slope of the ice sheet, while  $-0.82^{\circ}\text{C}$  per  $1^{\circ}$  of latitude was derived for the eastern slope. The mean annual lapse rate along the surface slope is  $0.71^{\circ}\text{C}$  per 100 m, with monthly mean lapse rates varying between  $0.4^{\circ}\text{C}$  per 100 m in summer and  $1.0^{\circ}\text{C}$  per 100 m in winter. The annual range of monthly mean temperatures is between  $23.5^{\circ}\text{C}$  and  $30.3^{\circ}\text{C}$  for the western slope of the ice sheet, with increasing ranges from south to north and with increase in elevation. The annual mean air temperature was found to be  $2^{\circ}\text{C}$  higher for the central part of Greenland for 1995–1999, compared to the standard decade 1951–1960.

In addition to providing climatological and glaciological observations from the field, further applications of the GC-Net data include the study of the ice sheet melt extent, which has been increasing over the last 2.5 decades; estimates of the ice sheet sublimation rate; reconstruction of long-term air temperature time series; assessment of surface climate; and the interpretation of satellite-derived melt features of the ice sheet. Potential applications for the use of the GC-Net

data are comparison of in-situ and satellite-derived surface parameters; operational weather forecasts; validation of climate models; and logistic support for ice camps and Thule AFB.

#### *Canadian Ice Caps*

Analysis of data from airborne laser surveys has shown that, much like the Greenland ice sheet, the Canadian ice caps appear to be losing mass in their ablating margins, while at their higher elevation accumulation zones they are either thickening slightly or remaining fairly constant. For most of the ice caps in the Queen Elizabeth Islands, this thinning can be explained by warm temperature anomalies during the late 1990s survey period. However, in the south, on Baffin Island, large thinning rates, on the order of a meter a year, do not seem to be related to any short-term temperature anomaly but rather are more likely a result of ongoing mass loss associated with deglaciation since the mini-ice age several centuries ago.

#### *Alaskan Glaciers*

Recent surveys of Alaskan glaciers has shown significant wastage, estimated to be about 30% of the total glacier contribution to sea level rise.

As a complement to this work, digital elevation models (DEMs) of Bagley Ice Valley and Malaspina Glacier produced by 1) Intermap Technologies, Inc. (ITI) from airborne interferometric synthetic aperture radar (InSAR) data acquired 4–13 September 2000, 2) the German Aerospace Center (DRL) from spaceborne InSAR data acquired by the Shuttle Radar Topography Mission (SRTM) 11–22 February 2000, and 3) the U.S. Geological Survey (USGS) from aerial photographs acquired in 1972–73, were differenced to estimate glacier surface elevation changes from 1972 to 2000. Spatially non-uniform thickening,  $10 \pm 7$  m on average, is observed on Bagley Ice Valley (an accumulation area), while non-uniform thinning,  $47 \pm 5$  m on average, is observed on the glaciers of the Malaspina complex (mostly an ablation area). Even larger thinning is observed on the retreating tidewater Tyndall Glacier. These changes have resulted from increased temperature and precipitation associated with climate warming and rapid tidewater retreat.

Work on Alaskan glaciers supported by NASA during 2003 included acquisition of small-aircraft laser altimeter data on selected glaciers and ice-fields of the St. Elias Mountains in south-central Alaska and Yukon. Profile data were acquired on seven glaciers that had not been measured



*Fjord near the Barnes Ice Cap on Baffin Island.*

previously, and repeat profile data were acquired on five glaciers that had been measured previously. The latter included the largest glacier systems in continental North America; that is, Bagley Ice Valley–Bering Glacier and the Seward–Malaspina Glacier systems, which have areas, including all tributaries, of about 5,200 and 5,000 km<sup>2</sup>, respectively. Repeat profile data were also acquired, and the position of the terminus was measured on Hubbard Glacier, which has been advancing and threatening to block the entrance to Russell Fjord. Ice dams caused by the advance of Hubbard Glacier have temporarily blocked this fjord entrance twice, in 1986 and 2002. If an ice dam forms that is strong enough to “hold,” the economy of the nearby community of Yakutat may be threatened by redirection of the drainage of the fresh water that now discharges into the Gulf of Alaska via the fjord mouth. An additional study of Alaskan glaciers has included detailed investigations into the mechanisms that control surging behavior.

### *Arctic Climate Modeling*

The goal of some of the more recent modeling efforts at NASA’s Goddard Institute for Space

Studies (GISS) was to investigate and develop more realistic sea ice/upper ocean models as part of the GISS GCM, with the ultimate purpose of improving the climate change forecast in the polar regions. Investigations focused on the model sensitivity to cavitating fluid and viscous–plastic dynamics; the oceanic mixing characteristics; and the viscosity diffusion models.

The primary improvement came from including the resistance to shear stress in the viscous–plastic dynamics: comparison to satellite data indicates much more realistic sea ice concentrations, thickness, and export through the Fram Strait. Reduced oceanic isopycnal mixing leads to reduced and thinner ice throughout the Arctic, while the viscosity diffusion produces expanded and thicker sea ice in the Arctic, both due primarily to their effect on North Atlantic Deep Water (NADW) production and associated heat transport. On the basis of these runs, composite experiments with the best combination of parameterizations were generated, which, besides affecting the sea ice, had influences of up to 4°C on atmospheric temperatures in the Arctic. Climate change experiments are underway to assess the polar region response with this new model.



*Polar stratospheric clouds, as seen from the NASA DC-8 over southern Sweden on January 14, 2003.*

## Atmospheric Chemistry

The SOLVE II Ozone Loss and Validation Experiment (SOLVE II) was a measurement campaign designed to examine the processes controlling ozone levels at mid- to high latitudes and acquire correlative data needed for the validation of the Stratospheric Aerosol and Gas Experiment (SAGE) III satellite measurements. SAGE-III is a NASA instrument aboard a Russian Meteor-3 satellite platform. SAGE-III is primarily used to measure high-latitude ozone loss.

The SOLVE II mission was primarily conducted during January 2003. Measurements were made in the Arctic high-latitude region during winter using the NASA DC-8 aircraft, as well as two heavy-lift

balloon flights, a number of smaller balloon packages, and ground-based instruments. The NASA DC-8 arrived in Kiruna, Sweden, slightly north of the Arctic Circle, on January 9, 2003. A total of 11 science flights were conducted in Kiruna, and the DC-8 returned to NASA Dryden on February 6, 2003.

Ozone loss in the polar stratosphere is directly caused by catalytic chlorine and bromine reactions. The high levels of reactive chlorine occur because of reactions of reservoir chlorine species on the surfaces of polar stratospheric clouds (PSCs). PSCs were observed by the NASA DC-8 lidar systems on the flights of January 9, 12, and 14 and February 4, 2003 at altitudes between 65,000 and 80,000 feet.

During the winter of 2002–2003, the polar vortex was cold and had moved southward toward Europe, exposing the air to sunlight. Normally ozone values in the core of the vortex near 20 km would be approximately 3 parts per million. However, because of the high levels of reactive chlorine, ozone steadily decreased over the course of the month. During early February, though, these values are near 1,500 ppbv, showing the very large ozone losses inside the polar vortex.

These initial results are only qualitative and will require further processing and quantitative analysis. These SOLVE II results will be directly used to quantify ozone loss in the vortex. The ozone values and ozone loss will then be compared to the SAGE III ozone values to validate our global observations of ozone.

*Ozone values observed on the flight from Kiruna, Sweden, to California on February 6, 2003. The x-axis of the figure shows the time, while the y-axis shows altitude. The polar vortex was situated over Kiruna (left side of the figure), such that the low ozone values at 20 km on the left are inside the polar vortex. Typically values of ozone inside the vortex in January would be near values of 3000 ppbv (the aqua color).*

